

AN EXPERIMENTAL INVESTIGATION INTO THE ARCHING EFFECT IN FINE SAND

J. Sadrekarimi and A.R. Abbasnejad*

Department of Geotechnical Engineering, University of Tabriz
Post Code 5166616471, Tabriz, Iran
jsadr@tabrizu.ac.ir - abbasnejad_ar@yahoo.com

*Corresponding Author

(Received: September 23, 2007 – Accepted in Revised Form: May 9, 2008)

Abstract In the current paper results of a well instrumented experimental procedure for studying the arching effect in loose and dense sand are presented. The apparatus comprises concentric circular trapdoors with different diameters that can yield downward while stresses and deformations are recorded simultaneously. As the trapdoor starts to yield, the whole soil mass deforms elastically. However, after an immediate specified displacement, depending on the diameter of the trapdoor and relative density of the soil, the soil mass behaves plastically. This behavior of sand occurs due to flow phenomenon and continues until the stress on trapdoor is minimized. Then the failure process develops in sand and the measured stress on the trapdoor shows an ascending trend. This indicates gradual separation of the yielding mass from the whole soil body. Finally, the flow process leads to establish a stable vault of sand called arching mechanism. Depending on the trapdoor diameter there is a critical relative density at/above which the test leads to form a stable arch. A mathematical method to establish the shape of the sand vault is introduced and the results obtained from experimental investigations are compared to this method. The results are also, compared to Terzaghi's theory and the assumption of upper boundary solution is discussed.

Keywords Arching Effect, Embankment, Relative Displacement, Stress Distribution

چکیده در این مقاله نتایج حاصل از بررسی پدیده قوس در ماسه شل و متراکم با استفاده از مدل فیزیکی ابزاربندی شده، نشان داده شده است. مدل فیزیکی مخزن پر از ماسه است که کف آن دارای دریچه‌های دایره شکل متحدالمرکز با اقطار مختلف می‌باشد که قابلیت حرکت به طرف پایین را دارند به طوری که مقادیر جابه‌جایی و تنش در زیر دریچه‌ها بطور همزمان قابل اندازه‌گیری می‌باشد. زمانی که دریچه شروع به پایین آمدن می‌کند، توده خاک بالای دریچه ابتدا بطور الاستیک جابه‌جا می‌شود. سپس، بعد از یک جابه‌جایی مشخص که مقدار آن بستگی به قطر دریچه و دانسیته نسبی ماسه دارد، توده رفتار پلاستیک از خود نشان می‌دهد. این رفتار ماسه که بدلیل بروز پدیده جریان به وقوع می‌پیوندد، تا آنجا که تنش روی دریچه به یک تراز حداقل میل کند، ادامه می‌یابد. آنگاه فرایند گسیختگی آغاز می‌گردد و تنش اندازه‌گیری شده روی دریچه به سمت یک مقدار معین رشد می‌کند تا این که گسیختگی در توده به وقوع بپیوندد. در این مرحله توده روی دریچه از توده ماسه مجاور جدا می‌گردد و سرانجام به ایجاد گنبدی پایدار (معروف به پدیده قوس)، می‌انجامد. با توجه به قطر دریچه مورد آزمایش، می‌توان یک دانسیته نسبی بحرانی تعریف کرد، به طوری که به ازای مقادیر بیش از آن، قوس پایدار به وجود می‌آید. روابط ریاضی برای به دست آوردن شکل گنبد ماسه‌ای ارائه شده و نتایج جمع‌آوری شده از آزمایش‌ها با این روش مورد مقایسه قرار گرفته است. همچنین نتایج، با تئوری ترزاقی و فرض تئوری کران پایین، مقایسه شده است.

1. INTRODUCTION

When part of a soil mass yields, while other part adjoining the yielding part remains stationary, movement between yielding and stationary parts causes shear stress to develop. This shear stress opposes the relative movement of soil masses.

Since the shearing resistance tends to keep the yielding mass in its original position, it reduces the pressure on the yielding part and increases it on the adjoining stationary part. The essential features of arching were demonstrated by Terzaghi performing experiments on sand with a yielding trapdoor. The shear plane theory was subsequently proposed by

him in 1943. The analysis involved studying the equilibrium horizontal element of soil, assuming that soil has perfectly plastic behavior. The equations that Terzaghi proposed for stress due to arching effect are [1]:

$$c > 0 \quad \text{and} \quad q = 0 \Rightarrow \sigma_v = \frac{B(\gamma - c/B)}{K \tan \phi} (1 - e^{-K \tan \phi z/B}) \quad (1)$$

$$c = 0 \quad \text{and} \quad q > 0 \Rightarrow \sigma_v = \frac{B\gamma}{K \tan \phi} (1 - e^{-K \tan \phi z/B}) + qe^{-K \tan \phi z/B} \quad (2)$$

$$c = 0 \quad \text{and} \quad q = 0 \Rightarrow \sigma_v = \frac{B\gamma}{K \tan \phi} (1 - e^{-K \tan \phi z/B}) \quad (3)$$

Where c is the coefficient of cohesion, q is surcharge pressure, $2B$ is trapdoor diameter, γ is the density of the soil, K is lateral pressure coefficient and z is the soil depth from the surface. Finn, et al [2] modified the plastic behavior assumption of Terzaghi and developed some experiments assuming the soil is linearly elastic. He obtained expressions for induced stresses in the mass of soil by vertical displacement and the rotation of a rigid strip. Borghignoli, et al [3] studied the arching effect in the soil over a flexible trapdoor and obtained expressions based on the relative stiffness between trapdoor and soil. Getzele, et al [4] used models composed of aluminum blocks with various shapes that were buried in coarse sand and a uniform pressure was applied to the surface of the sand. The blocks were connected to a ring that served as a flexible support for the model and as a gouge for the total vertical force applied to the structure. After the cylinder was buried in the sand, a uniform pressure was applied on the surface of the sand and the normal force acting on each segment was measured by load cells. Hoeg, et al [5] designed a model tunnel with a rigid steel cylinder, split longitudinally into 12 segments. After the cylinder was buried in the sand, a uniform pressure was applied on the surface of the sand and the normal force acting on each segment was measured by load cells. Clough, et al [6] applied the finite element method to

analyze retaining wall behavior using various assumptions regarding the characteristics of the interface between a wall and backfill. Atkinson, et al [7] examined the behavior of the shallow tunnels in dry sand using a tunnel model, lined with a thin rubber membrane in both laboratory situation under gravity acceleration and centrifuge with 75 g acceleration. The tunnel was constructed initially with an inner pressure equal to the overburden weight, which was then reduced in decrements until the tunnel collapsed. Then they compared the experimental results with the upper and lower boundary theory. The results showed that the upper and lower boundary theory has proper accuracy to estimate the loads applied to the lining of the tunnel. Koutsabeloulis, et al [8] studied the stress distribution around a trapdoor due to arching effect using finite element method. Ono, et al [9] studied the arching effect in the soil mass around a tunnel and behind a retaining wall using rubber membrane filled with air under pressure equal to that applied from soil, then the pressure decreased until the air was extracted. The results then were compared with the ones obtained from theoretical study assuming equilibrium of an arbitrary soil element. Hashash, et al [10] presented a detailed interpretation of the evolution of stresses around a braced excavation in a deep layer of soft clay. The results provided a new insight for explaining the development of lateral earth pressures for braced excavations and give a quantitative illustration of conceptual load transfer mechanisms and soil arching. The boundaries of the arching zones for both single tunneling and parallel tunneling were determined by Lee, et al [11]. The prediction of tunneling-induced ground movements during excavation of soft ground tunnel has been carried out using various methods, including empirical methods derived from field observations [12] and centrifuge modeling [13,14], or numerical methods [15]. Park, et al [16] performed model tests under 1g conditions to simulate tunneling events in unconsolidated ground with various levels of inclined layers. They found that remarkable non-symmetrical distributions of the earth pressure arose when a tunneling event took place in an inclined layer with 60° inclination. Stone and Newson, et al [17] presented the results of a series of centrifuge tests designed to investigate the effects of arching on soil-structure interaction.

Continuum approaches to describe the stress dip under sand piles can be found in Wittmer, et al [18], Savage [19] and Didwania, et al [20], and a comprehensive review of continuum efforts was presented by Savage [21]. Michalowski, et al [22] focused on the limit analysis approach and admissible radial stress fields in prismatic sand piles. In spite of vast investigations on soil arching, there hasn't been an ample study done on the parameters affecting arching mechanism in a soil mass and the stress, strain path. Current paper presents results of an experimental work in which variations of normal stress exerted by circular trap doors are monitored while they were yielded downward gradually.

2. PROCEDURE

2.1. Soil Properties The test soil was a cohesionless silty sand with No. 10 and No. 200 sieve passings 100 % and 9 %, respectively. The gradation curve coefficient of curvature C_c and coefficient of uniformity C_u were 1.1 and 5.3, respectively. The sieve test result is introduced in Figure 1. The specific gravity of solid particles was 2.61 and the moisture content was kept at 3 %

throughout the experiments. The soil was classified as SP-SM according to USCS. The maximum and minimum dry densities were measured as 16.77 and 12.26 kN/m^3 , respectively. In order to determine shear strength parameters corresponding to the relevant stress levels, direct shear tests under 1.62 and 11.23 kPa surcharges were carried out. The results are illustrated in Figures 2 and 3. The magnitude of the internal friction angle ϕ depends on the magnitude of the state of the stress for a particular soil [7]. The lower the normal load the higher the ϕ angle.

2.2. The Model Properties An apparatus was designed and constructed. The whole system is schematically shown Figure 4. The sand container was 0.358 m^3 in volume and 60 cm in height with an octagonal horizontal cross section with a 98 cm diameter circumferential circle. The container was made of 4 mm thick steel plate strengthened with stiffeners. Three concentric circular trapdoors mounted under the base of the container, as shown in Figures 4 and 6. The trapdoors were 10, 20 and 30 cm in diameter which could yield downward separately by a very sophisticated computerized system as shown in Figures 4 to 6. The load magnitudes on the trapdoors, caused by the pressure of the overburden soil, were measured

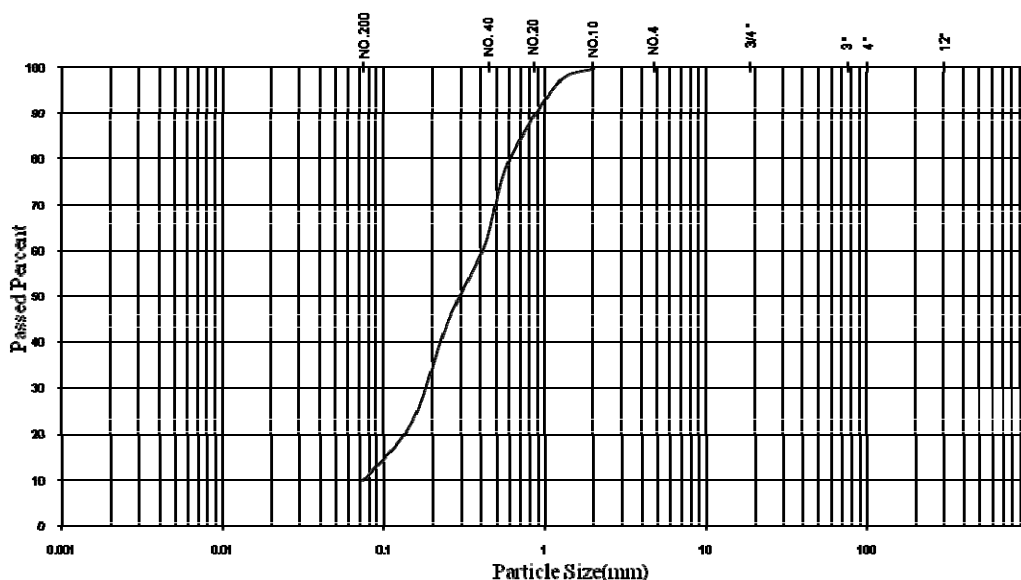


Figure 1. Sieve analysis of the test soil.

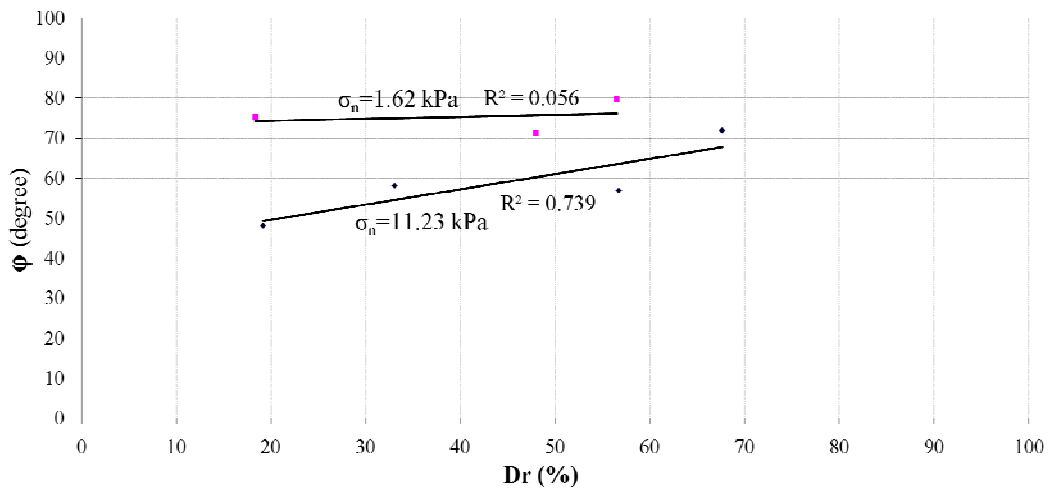


Figure 2. Internal friction angle ϕ against relative density.

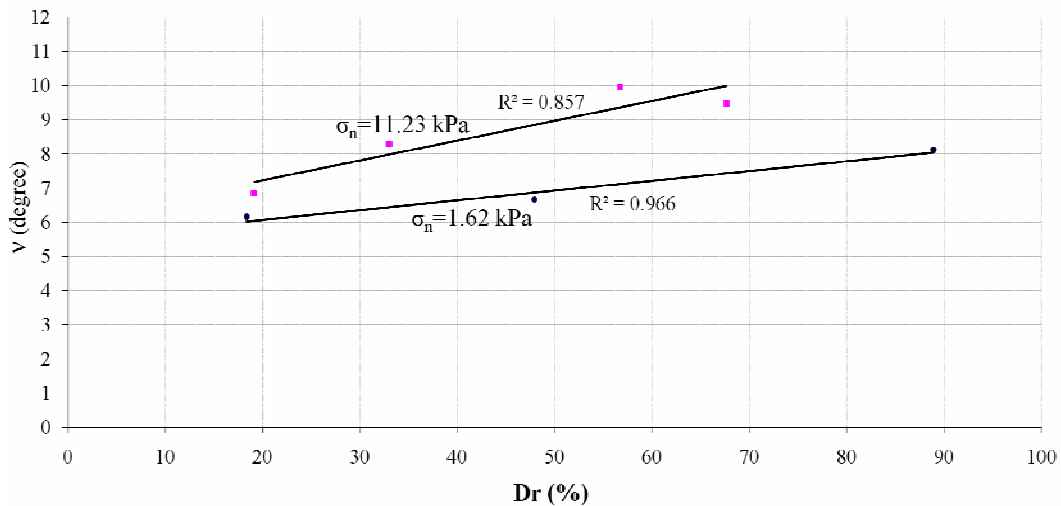


Figure 3. Dilation angle v against relative density.

using a load cell. The displacement of the trapdoors and also the surface of the soil due to trapdoor yielding all were monitored using Linear Variable Differential Transformer (LVDT) installed under the platform and over the soil surface.

2.3. Test Procedure At the beginning, without any displacement, the normal stress σ_o applied to the trapdoor is γh , in which γ is the density of the sand and h is the height of the mass of the sand in

the container. In order to deposit the sand in loose condition it was poured from a defined height through a sieve No. 10; and in order to produce dense sand each layer of sand was compacted evenly with a 4.54 kg rammer. Each layer of soil was 5 cm thick, and the height of falling rammer and number of blows were varied depending on the expected densities. This stage was very time consuming and several tests were carried out to make sure that the soil density was the same throughout the whole mass.

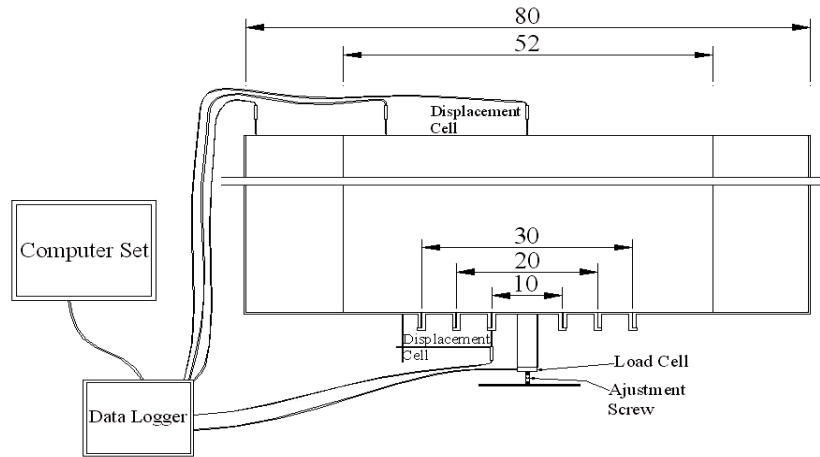


Figure 4. Schematic diagram of the apparatus.



Figure 5. General view of the test system.



Figure 6. Detail of the trapdoors, load cell and displacement gauge.

Having filled the container with sand, the nuts and bolts holding the trapdoor were unscrewed while the upward pressure on the trapdoor was being adjusted so that the trapdoor did not displace. This was a curtail point of course. At this stage the recorded stress was very close to γh . Following this stage the trapdoor was slowly yielded downward with loosening the major screw of the load cell. This trend continued until the load displayed by the load cell tended towards an asymptote.

3. RESULTS

The test results with 10, 20 and 30 cm diameter trapdoors are depicted in Figures 7, 8 and 9. In these figures the σ/σ_0 is the ratio of normal stress applied on the trapdoor during any stage of yielding to the same stress at the initial state of trapdoor with no displacement. This stress ratio defines stress reduction level due to arching effect, indeed. ΔH is the trapdoor downward yield.

4. DISCUSSION

4.1. The Main Aspects of the Phenomenon

Referring to Figures 7 to 9 it is observed that at the early stages of the tests, stress applied on the trapdoor due to soil weight decreases sharply as it yields. At this stage the whole mass of sand behaves mostly elastic. As the trapdoor yield proceeds, the stress ratio decreases and tends toward a minimum value and then increases again until it tends toward an ultimate constant level. This trend is true for all trapdoors. However, as the diameter of the trapdoor increases and/or the sands' relative density decreases, the minimum and ultimate stress ratios both increase. This behavior may be interpreted as follows. As the trapdoor yield starts the overlying soil weight, exerted by the trapdoor, is transmitted gradually onto the container base, surrounding the trapdoor. For this reason at initial stage of the test, in which the sand mass behaves mostly elastic, a small yield is followed by a sharp decrease in the stress carried by the trapdoor. As the trapdoor yield proceeds,

random plastic points in the sand mass deforms. At this stage stress adjustment due to trapdoor yielding is not immediate and occurs with some time lag. This is attributed to the flow phenomenon that occurs due to the plastic behavior of the yielding sand mass. Then continuing the downward displacement, and the stress ratio approaching a minimum value, failure occurs. At failure state, depending on the trapdoor diameter, relative density, and the dilation angle of the sand, the failing sand mass dilates, which imposes further stress on the trapdoor and continues until the failure surface has developed and the yielded mass of sand is separated from the whole mass. Following this stage there is no longer any stress or mass exchange between two parts. Accordingly, the load cell displays a constant value. It was observed that as the sands' relative density decreased to a specified value, no stable arch was established and the failure surface developed up to the sand mass surface. A representative stable arch for 20 cm trapdoor diameter and relative density of $D_r = 38.60\%$ is shown in Figure 10.

Referring to Figures 7 to 9, the ultimate stresses applied to the trapdoor are determined and plotted against relative density in Figure 11. It is observed that the ultimate stress ratio on the trapdoor generally decrease as the relative density increases. However, up to a certain D_r value, say 28 % for 20 cm diameter, no stable arch is established. As the relative density increases the failure mode changes from sand flow to arch formation. In fact, there is a relative density boundary that defines the formation of stable arch. As the relative density increases, the stress approaches to a minimum value. At this relative density, the pressure applied to the buried trapdoor is minimum. Line B may be adopted as the stable and unstable arch boundary. As the soil relative density increases the stress on the trapdoor also increases and tends toward an asymptote. In other words, relative density increment has no longer any effect on the stress applied on the trapdoor. This behavior is true for cases that the stress on the trapdoor is minimum. Line A, however, may be referred to as a line that points out minimum stress ratio. It shows that at $D_r = 39\%$ the stress ratio tends to be a minimum value. Probably this is due to the fact that, as the D_r value exceeds 39 % the soil density increases and causes the soil mass to collapse. Figure 12

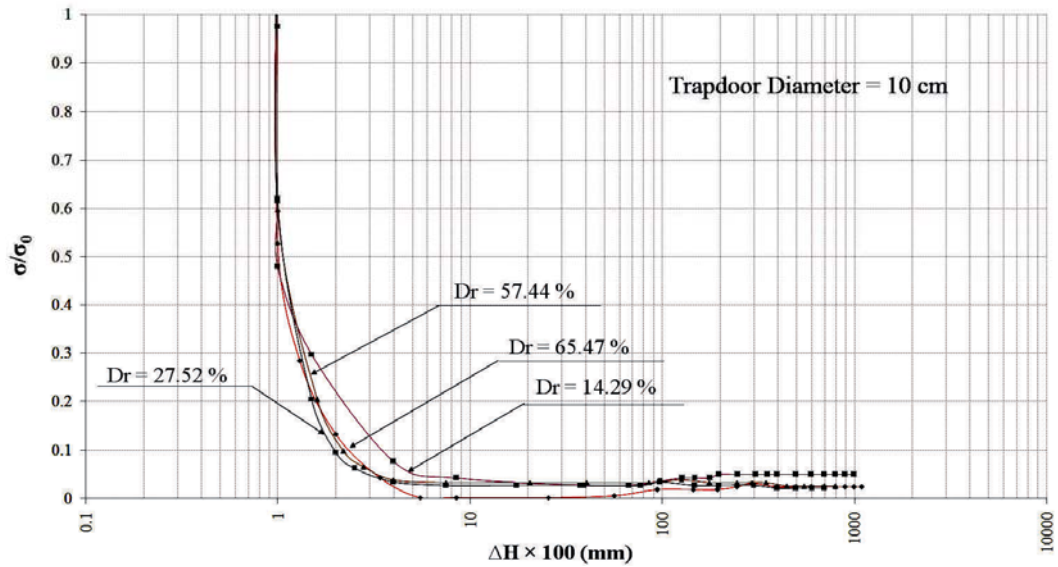


Figure 7. Stress ratio-yield plots for 10 cm trapdoor diameter.

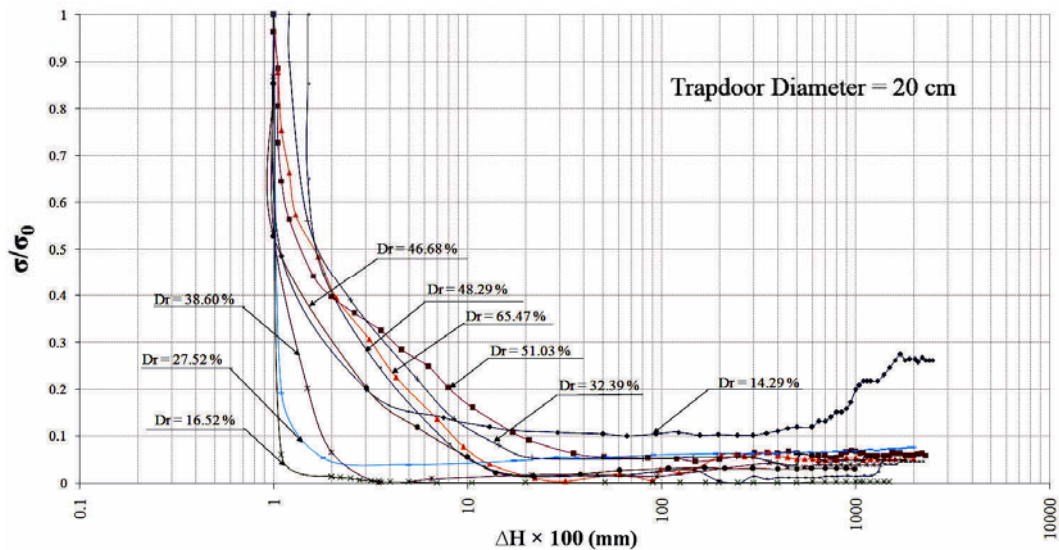


Figure 8. Stress ratio-yield plots for 20 cm trapdoor diameter.

illustrates the pressure imposed on the trapdoor against the relative density of the sand. In this case, similar to the ultimate stress case, the critical and minimum relative density may be defined.

4.2. Mathematical Approach In order to establish the best equation to fits the shape of sand arch, the pictures taken during the experimental

works were investigated. In Figure 13, the sand arch picture for 20 cm trapdoor diameter and 14.21 kN/m³ dry density (Dr = 51.03 %) is shown. This figure was selected as a representative case and the second to fourth order equations were examined for the best fit. As shown in this figure, it was observed that with the fourth order equation the best coincidence is achieved. Referring to the fact

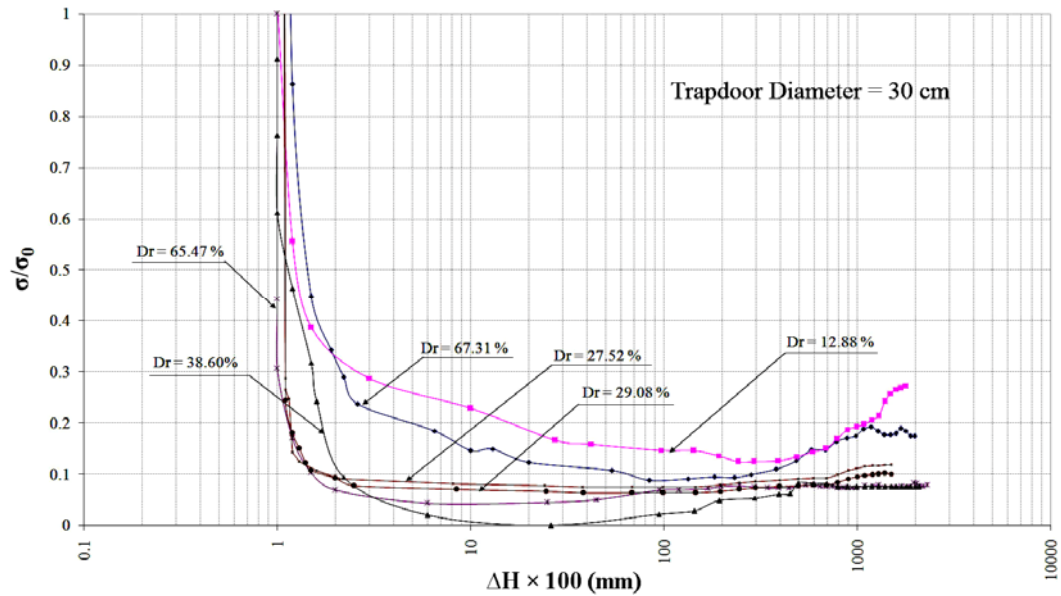


Figure 9. Stress ratio-yield plots for 30 cm trapdoor diameter.

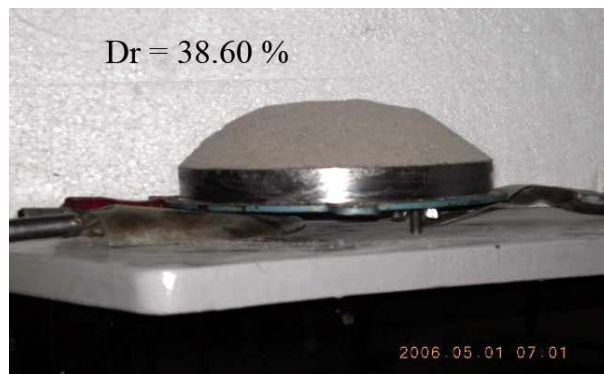


Figure 10. Stable arch for 20 cm diameter trapdoor.

that the arch shape is symmetric, the general fourth order governing equation is set to $z = Ax^4 + Bx^2 + C$. The mathematical model of the arch is shown in Figure 14.

According to the boundary condition:

$$z = Ax^4 + Bx^2 + C$$

$$\left\{ \begin{array}{l} z = h, x = 0 \rightarrow c = h \end{array} \right.$$

$$\left\{ \begin{array}{l} x = D/2, z = 0 \rightarrow \frac{AD^4}{16} + B\frac{D^2}{4} + h = 0 \end{array} \right.$$

Then:

$$B = \frac{-4h}{D} - \frac{AD^2}{4}$$

The volume under the surface of the arch (V) is obtained from:

$$V = 2\pi \int_a^b x \cdot F(x) dx$$

From which:

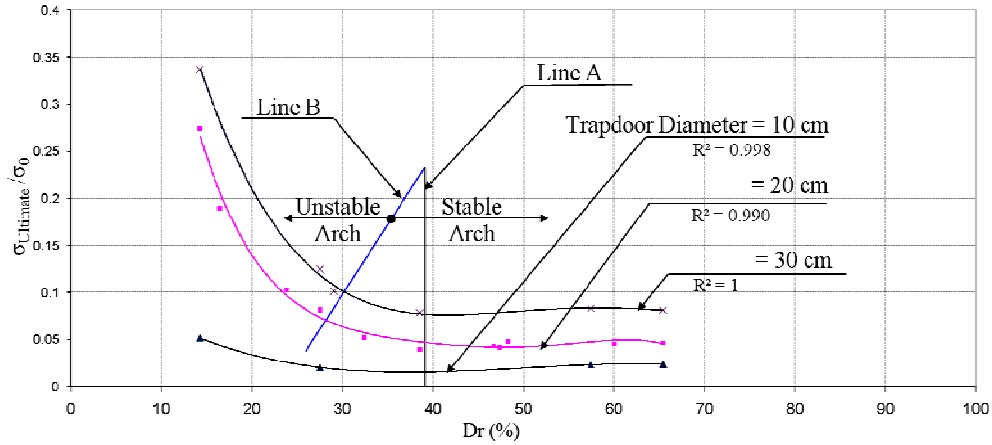


Figure 11. Ultimate stress ratio-relative density plots.

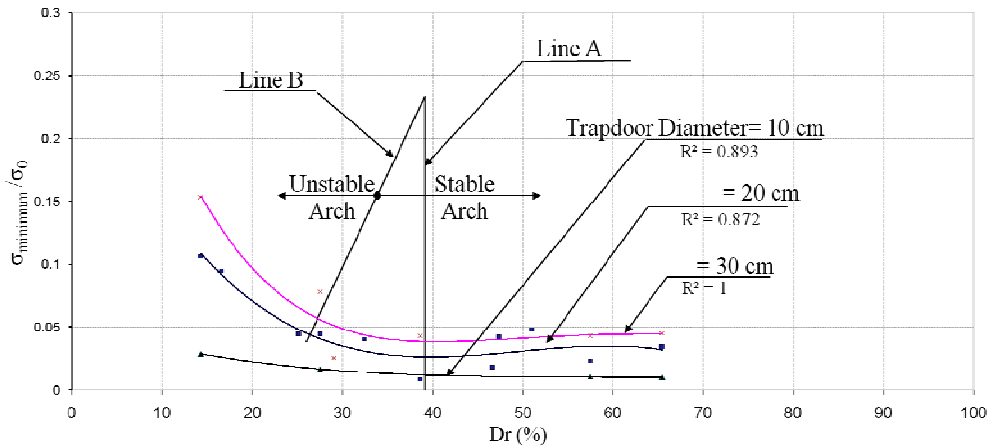


Figure 12. Minimum stress ratio-relative density plot.

$$V = \frac{D^2}{8\pi} \left(h - \frac{AD^4}{48} \right)$$

$$\gamma = \gamma_d(1+m)$$

The stress applied onto the trapdoor is:

Then the general equation of the ultimate stress applied onto the trapdoor will be as:

$$W = \gamma V, \sigma_V = \frac{W}{A} = \frac{\gamma V}{A}$$

$$\sigma_V = \frac{\gamma_d(1+m)}{2} \left(h - \frac{AD^4}{48} \right)$$

$$\sigma_V = \frac{\frac{\gamma D^2}{8\pi} \left(h - \frac{AD^4}{48} \right)}{\frac{\pi D^2}{4}} = \frac{\gamma}{2} \left(h - \frac{AD^4}{48} \right)$$

For 3 % moisture content the stress level will be as:

$$\sigma_V = \frac{1.03 \gamma_d}{2} \left(h - \frac{AD^4}{48} \right)$$

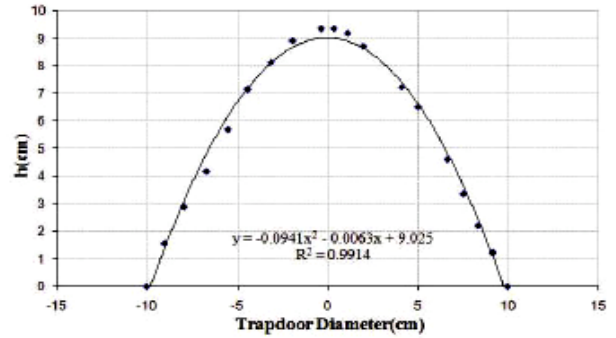
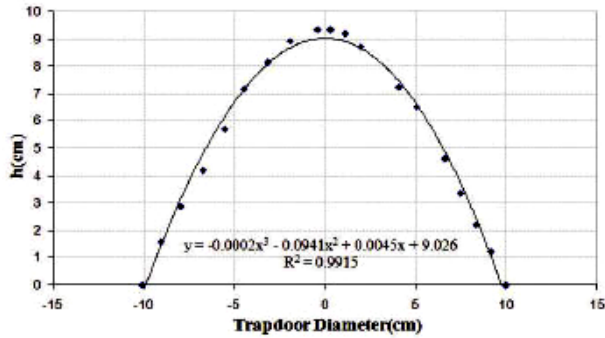
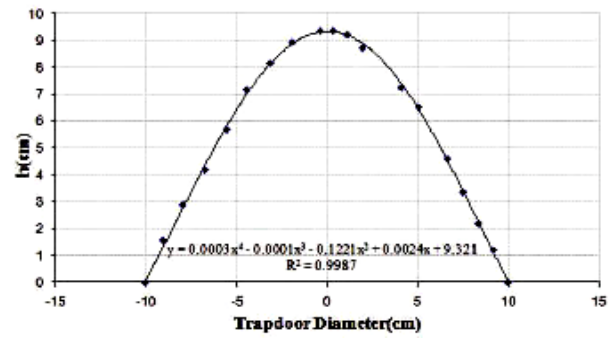


Figure 13. Comparing the results of the interpolation of the arches.

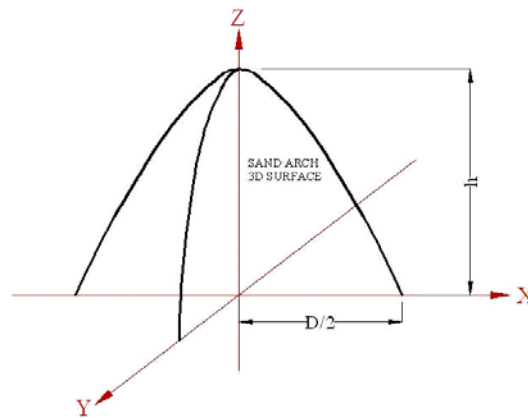


Figure 14. Mathematical model of the arch.

Then, the 3D equation of the of the arch boundary surface will be as:

$$z = \frac{A}{2}(x^4 + y^4) - \left(\frac{zh}{D^2} + \frac{AD^2}{8} \right) (x^2 + y^2) + h$$

Using the sand arch pictures provided during the

experimental works and mathematical manipulations, the coefficients A and h are determined and plotted against relative density in Figures 15 and 16. The yielded sand mass volumes obtained from these equations and also directly from the tests, are summarized in Table 1.

Referring to Table 1 it is observed that, the arch volumes obtained from experiment and calculation

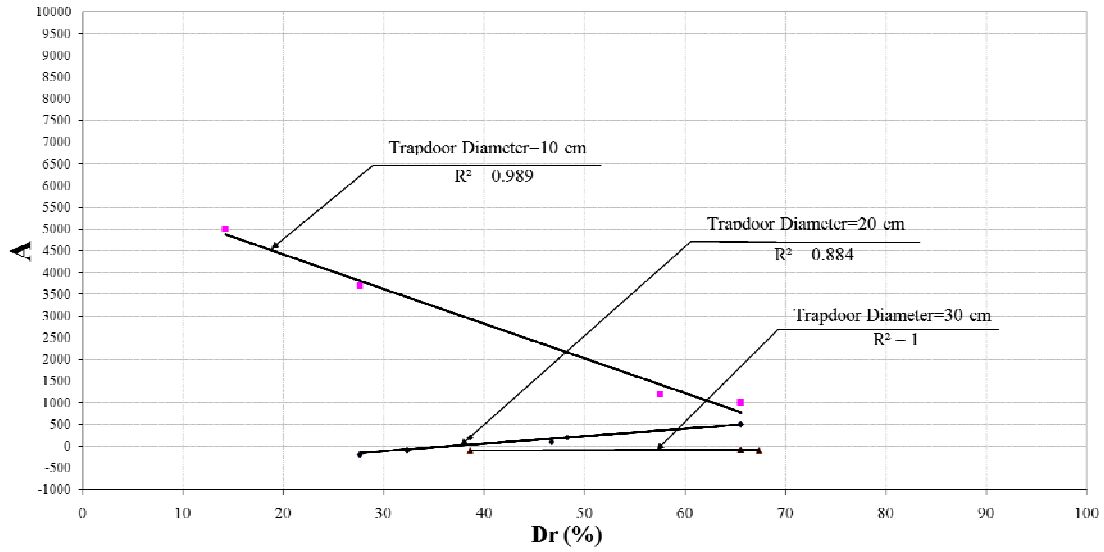


Figure 15. The A coefficient-relative density plot.

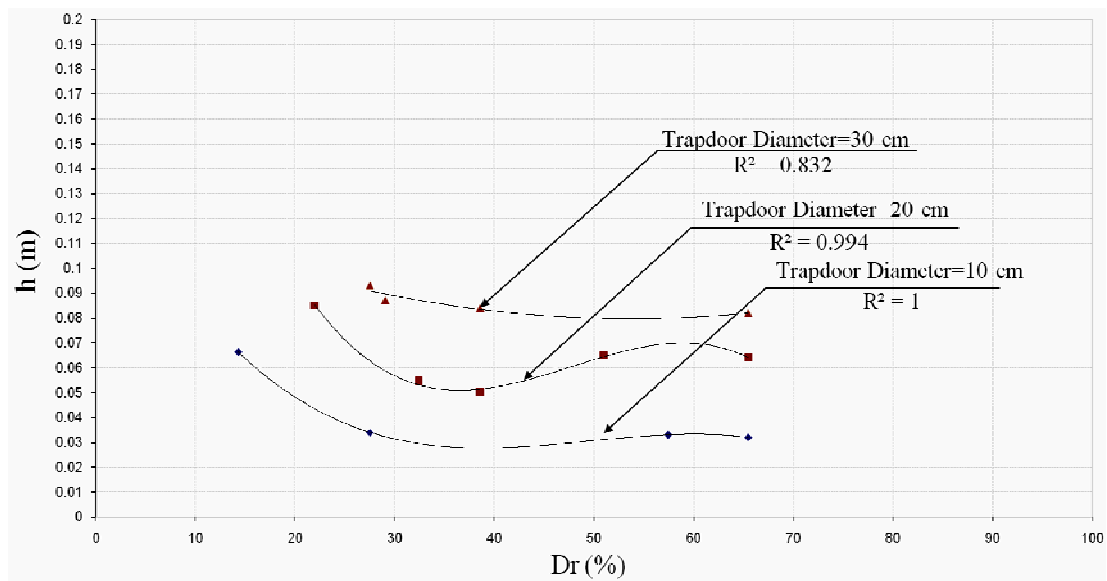


Figure 16. The h coefficient-relative density plot.

are quite close with an average error in the order of $\Delta V/V_1 = 5.5\%$. This proves that the precision of the mathematical approach of arch shape is in an acceptable order.

4.3. Comparison of the Experimental Results with Terzaghi's Theory

Referring to

the Terzaghi's procedure, as explained above, the stress ratios applied to the trapdoors were calculated for different relative densities of sand and are shown in Figure 17. In order to carry out calculations, the equation No. 3 that was introduced in the introduction of this paper, was employed.

TABLE 1. Comparing the Volume of Arches Obtained from Calculation and Experimental Results.

Trapdoor Diameter (m)	Wet Density of Sand (kN/m ³)	Dry Density of Sand (kN/m ³)	A	h	V ₁ = Volume of arch from Calculation (m ³) × 10 ³	Weight of Sand Arch from Experimental Results(kN)	V ₂ = Volume of Arch from Experiment (m ³) × 10 ³	ΔV/V ₁ %
0.10	13.13	12.75	5000	0.067	0.2221	0.0031	0.2361	6.30
0.10	15.33	14.88	1000	0.032	0.1174	0.0017	0.1109	-5.54
0.10	13.64	13.24	3700	0.035	0.1071	0.0013	0.0953	-11.02
0.10	14.94	14.50	1200	0.032	0.1158	0.0015	0.1004	-13.30
0.20	14.64	14.21	0	0.065	1.0205	0.0151	1.0322	1.15
0.20	15.33	14.88	500	0.064	0.7431	0.0129	0.8414	13.23
0.20	14.09	13.67	200	0.05	0.6803	0.0102	0.7240	6.42
0.20	14.44	14.02	100	0.06	0.8897	0.0113	0.7837	-11.91
0.20	14.51	14.09	200	0.061	0.8530	0.0127	0.8747	2.54
0.20	13.83	13.43	-100	0.055	0.9158	0.0129	0.9327	1.85
0.20	13.64	13.24	-100	0.085	1.4392	0.0199	1.4662	1.88
0.30	15.33	14.88	-80	0.082	3.3735	0.0516	3.3656	-0.23
0.30	15.42	14.97	-100	0.082	3.4928	0.0509	3.3005	-5.51
0.30	14.09	13.68	-100	0.084	3.5634	0.0458	3.2503	-8.79

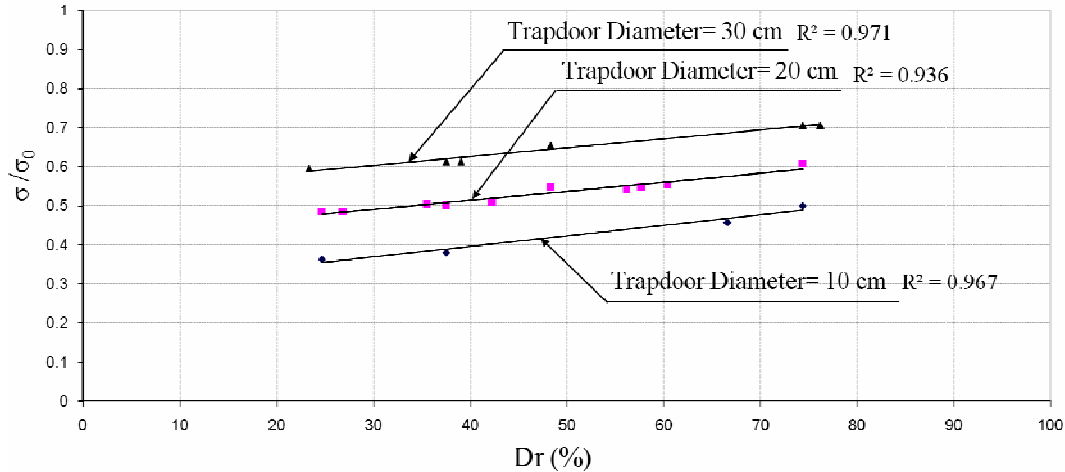


Figure 17. Stress applied onto the trapdoor obtained from Terzaghi's theory.

The coefficient of cohesion c is set to zero and there is no surcharge pressure on the sand, so $q = 0$, and B is the trapdoor diameter. For each test σ_v was obtained from this equation. Note that according to the Terzaghi's method the soil mass resting at above 2.5 times of a trapdoor diameter is assumed as surcharge. Referring to Figure 17, it is seen that the stress ratio σ/σ_0 increases as the sand relative density increases. Also comparing Figure 17 with Figures 7 to 9 reveals that the stress values obtained from the Terzaghi's theory are corresponding to the stress values measured at low strains, say $\Delta H \ll 0.1$ mm.

4.4. Comparing the Results with the Upper Boundary Theory In lower boundary theory, it is assumed that the soil behaves in elastic condition and there is not any failure in the soil mass. However, in upper boundary theory a complete failure in soil mass is assumed so that the failure surface above tunnel shapes a cone with $2v$ vertex angle, in which v is the dilation angle of the soil [7]. In Figure 18 the departed soil cones with $2v$ and 2ϕ vertex angles and those obtained from the current experiment are depicted in which v and ϕ are soil dilation and internal friction angle, respectively. It is seen that the theoretical cones with $2v$ vertex angle are very conservative, as they are quite distinct from the experimental vaults. It appears that it would be more logical if the vertex angle was taken as 2ϕ

rather than $2v$, although with 2ϕ angle the load due to arching is somewhat underestimated.

4.5. Sand Mass Surface Settlement Ultimate settlements in the center of sand mass surface due to trapdoors yielding are plotted in Figure 19 against relative density. It is observed that for all three trapdoors sand surface settlement decreases gently and tends towards a negligible value as the relative density increases. The best fit curves are shown in this figure and are third order functions. It appears that for a defined thickness of sand mass and trapdoor diameter there is a relative density at and above ground surface settlement, due to arching effect is negligible.

5. SUMMARY AND CONCLUSIONS

- Relative density of the soil and the trapdoor diameter, both are dominant factors affecting formation of a stable arch. As the trapdoor yields, following a small initial mostly elastic strain, the soil mass deforms plastically with larger strain rates and pressure applied onto the trapdoor decreases to a minimum value. Then, as the trapdoor yield continues, depending on the dilation angle and relative density of sand, stress

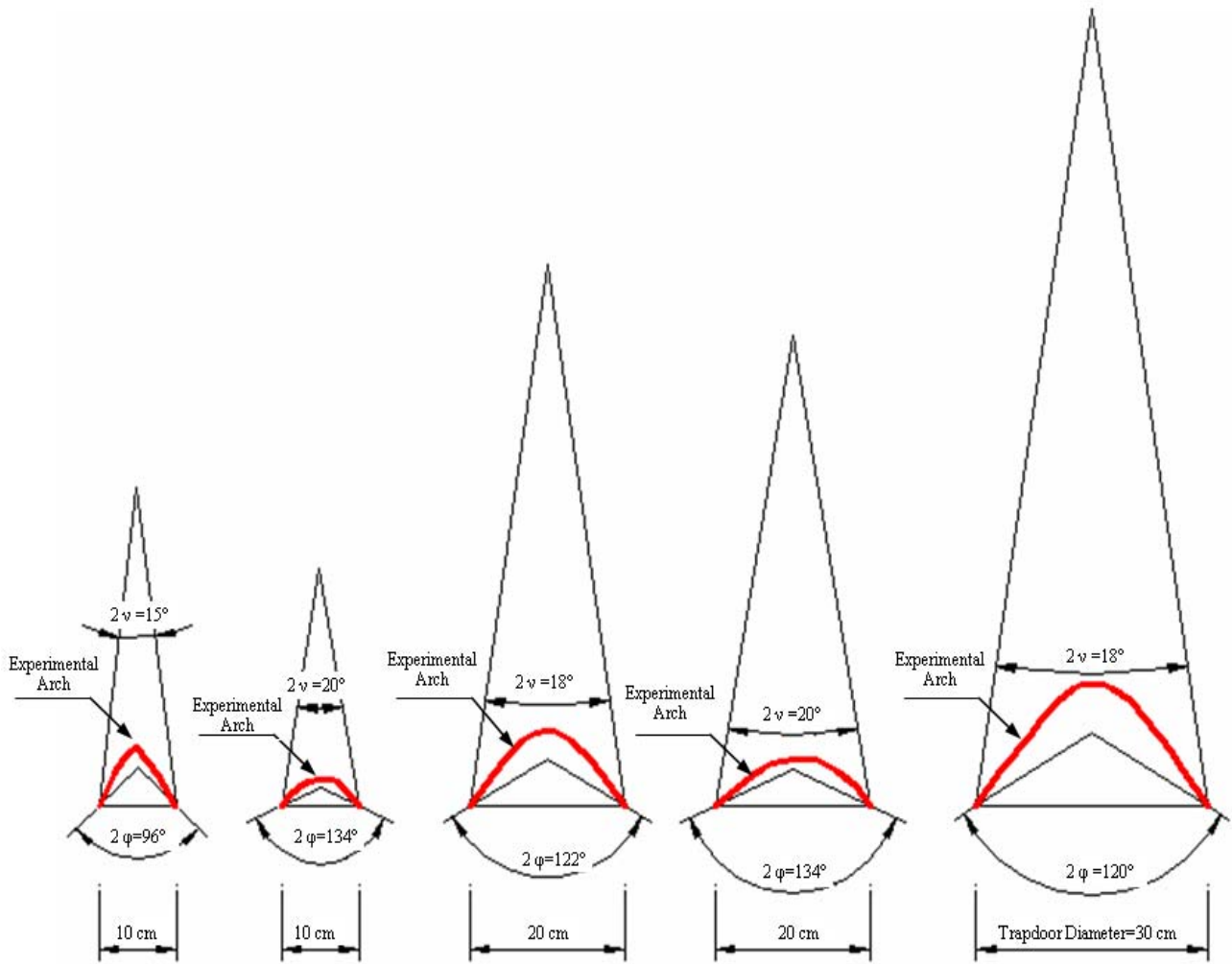


Figure 18. Comparison of cones with $2v$ and 2ϕ vertex angles with test results.

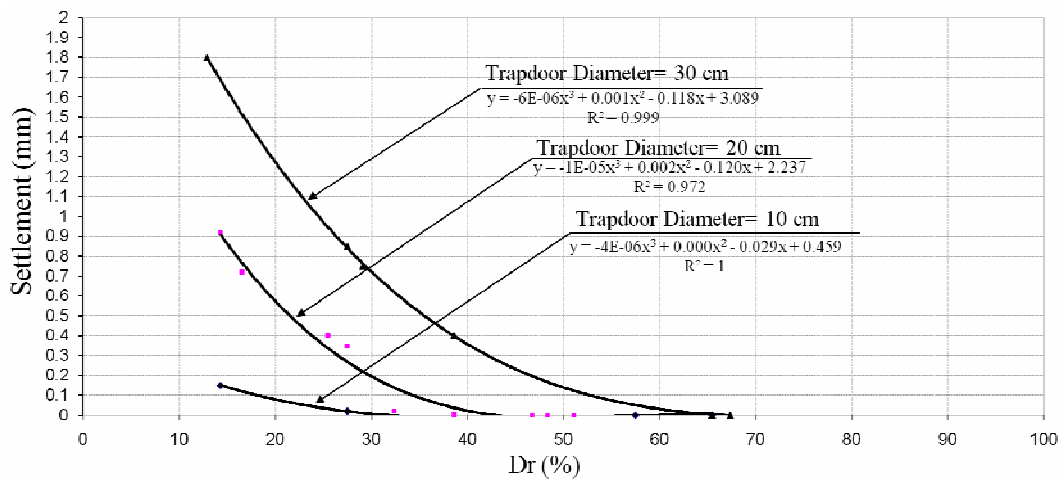


Figure 19. Ultimate settlement of sand surface due to trapdoor yielding.

level on the trapdoor increases gently and finally tends towards a constant value. At this stage the yielding sand mass separates from the whole mass.

- There is a critical relative density below which no stable arch is established. Also, there is an optimum relative density at which the stress applied onto the trapdoor is a minimum value. Above this relative density the stress level gently increases and ultimately tends towards a constant value (Figures 11 and 12).
- As the trapdoor yields, an upper and lower boundary for the stress applied onto the trapdoor can be defined.
- With Terzaghi's theory the stress ratio σ/σ_0 increases as the relative density increases, however, the current work proves that the ultimate stress decreases as the soil relative density increases. This may be attributed to the fact that the stress values obtained from Terzaghi's theory correspond to very low displacements.
- Comparing the results with the upper boundary theory, it is seen that the theoretical cones with 2ψ vertex angle are conservative, as they are quite distinct from the experimental vaults. It appears that it would be more logical if the vertex angle was taken as 2ϕ rather than 2ψ .
- For each thickness of sand mass and trapdoor diameter there is a relative density at and above which, the ground surface settlement due to arching effect becomes practically negligible.

6. REFERENCES

1. Terzaghi, K., "Theoretical Soil Mechanics", John Wiley and Sons, Inc New York, U.S.A., (1943).
2. Liam Finn, W. D., "Boundary Value Problems of Soil Mechanics", *J. Soil Mech. Fdns Div. Am. Soc. Civ. Engrs.*, Vol. 89, (1963), 39-72.
3. Burghignoli, A., "Soil Interactin in Buried Structures", *Source: Proceeding of the International Conference on Soil*, (Univ of Rome, Italy), Vol. 2, (1981), 69-74.
4. Getzler, Z., Komornik, A. and Maturik, A., "Model Study on Arching Above Buried Structures", *J. Soil Mech. Fdns Div. Am. Soc. Civ. Engrs.*, Vol. 94, (1968), 1123-1141.
5. Hoeg, K., "Stresses Against Underground Structural Cylinders", *J. Soil Mech. Fdns Div. Am. Soc. Civ. Engrs.*, Vol. 94, (1968), 833-858.
6. Clough, G. W. and Duncan, J. M., "Finite Element Analyses of Retaining Wall Behaviour", *J. Soil Mech. Fdns Div. Am. Soc. Civ. Engrs.*, Vol. 97, (1971), 1657-1673.
7. Atkinson, J. H. and Potts, D. M., "Stability of a Shallow Circular Tunnel in Cohesionless Soil", *Gkotechnique*, Vol. 27, No. 2, (1977), 203-215.
8. Kouthabeloulis, N. C. and Griffiths, D. V., "Numerical Modelling of the Trapdoor Problem", *Geotechnique*, Vol. 39, No. 1, (1989), 77-89.
9. Ono, K. and Yamada, M., "Analysis of Arching Action in Granular Mass", *Geotechnique*, Vol. 43, No. 1, (1993), 105-120.
10. Hashash, Y. M. A. and Whittle, A. J., "Mechanism of Load Transfer and Arching for Braced Excavation in Clay", *Journal of Geotechnical and Geo Environmental Engineering*, Vol. 128, No.3, (March 1, 2002), 187-197.
11. Lee, C. J., Chiang, K. H. and Kou, C. M., "Ground Movement and Tunnel Stability when Tunneling in Sandy Ground", *Journal of the Chinese Institute of Engineers*, Vol. 27, No. 7, (2004), 1021-1032.
12. Clough, G. W. and Schmidt, B., "Design and Performance of Excavation and Tunnels in Soft Clay", *Soft Clay Engineering*, Elsevier, Amsterdam, Netherlands, Chapter 8 (1981), 600-634.
13. Mair, R. J., "Centrifugal Modeling of Tunnel Construction in Soft Clay", Ph.D Thesis, University of Cambridge, Cambridge, CB3, U.K., (1979).
14. Wu, B. R. and Lee, C. J., "Ground Movements and Collapse Mechanisms Induced by Tunneling in Clayey Soil", *International Journal of Physical Modeling*, Vol. 3, No. 4, (2003), 13-27.
15. Lee, K. M. and Rowe, R. K., "An Analysis of three Dimensional Ground Movements: the Thunder Bay Tunnel", *Canadian Geotechnical Journal*, Vol. 28, No. 1, (1991), 25-41.
16. Park, S. H. and Adachi, T., "Laboratory Model Tests and FE Analyses on Tunneling in the Unconsolidated Ground with Inclined Layers", *Tunneling and Underground Space Technology*, Vol. 17, (2002), 181-193.
17. Stone, K. J. L. and Newson, T. A., "Arching Effects In Soil-Structure Interaction", *Phillips, Geo, Oopescu (Eds.), Physical Modeling in Geotechnics*, ICPMG 02, (2002), 935-939.
18. Wittmer, J. P., Cates, M. E. and Claudin, P., "Stress Propagation and Arching in Static Sand Piles", *J. Phys. I France*, Vol. 7, (1997), 39-80.
19. Savage, S. B., "Problems in the Statics and Dynamics of Granular Materials", *Powders and Grains 97*, Behringer, R. P. and Jenkins, J. T., Eds., (1997), 185-194.
20. Didwania, A. K., Cantelaube, F. and Goddard, J. D., "Static Multiplicity of Stress States in Granular Heaps", *Proc. Roy. Soc. London*, Vol. A 456, (2000), 2569-2588.
21. Savage, S. B., "Modeling and Granular Material

Boundary Value Problems”, Physics of Dry Granular Media Herrman, H. J., Hovi, J.-P. and Luding, S., Eds., Kluwer Acad Press, (1998), 25-95.

22. Michalowski, R. L. and Park, N., “Admissible Stress Fields and Arching in Piles of Sand”, *Geotechnique*, Vol. 54, No. 8, (2004), 529-538.